frontiers | Frontiers in Earth Science

TYPE Original Research
PUBLISHED 16 April 2024
DOI 10.3389/feart.2024.1347252

Check for updates

OPEN ACCESS

EDITED BY
Muhammad Idrees,
University of Science and Technology of China, China

REVIEWED BY
Michela Giustiniani,
National Institute of Oceanography and Applied Geophysics, Italy
Emanuele Lodolo,
National Institute of Oceanography and Applied Geophysics, Italy

*CORRESPONDENCE
Shyam Chand,
shyam.chand@ngu.no

RECEIVED 30 November 2023
ACCEPTED 21 March 2024
PUBLISHED 16 April 2024

CITATION
Chand S, Knies J, Geissler WH, Plaza-Faverola A and Thorsnes T (2024), Acoustic evidence of hydrocarbon release associated with the Spitsbergen Transform Fault, north of the Molloy Ridge, Fram Strait. *Front. Earth Sci.* 12:1347252. doi: 10.3389/feart.2024.1347252

COPYRIGHT
© 2024 Chand, Knies, Geissler, Plaza-Faverola and Thorsnes. This is an open-access article distributed under the terms of the Creative Commons Attribution License (CC BY). The use, distribution or reproduction in other forums is permitted, provided the original author(s) and the copyright owner(s) are credited and that the original publication in this journal is cited, in accordance with accepted academic practice. No use, distribution or reproduction is permitted which does not comply with these terms.

Acoustic evidence of hydrocarbon release associated with the Spitsbergen Transform Fault, north of the Molloy Ridge, Fram Strait

Shyam Chand[1]*, Jochen Knies[1,2], Wolfram H. Geissler[3], Andreia Plaza-Faverola[2] and Terje Thorsnes[1]

[1]Geological Survey of Norway (NGU), Trondheim, Norway, [2]Department of Geosciences, iC3: Centre for ice, Cryosphere, Carbon and Climate, UiT The Arctic University of Norway, Tromsø, Norway, [3]Alfred Wegener Institute, Helmholtz Centre for Polar and Marine Research (AWI), Bremerhaven, Germany

Hydrocarbon gases formed from biotic and abiotic processes are released through the seafloor at different locations around the world. They have been widely observed directly in video and photo data, and indirectly on echosounder data. Even though biotic gas generation is a very common process, abiotic gas generation is limited to regions where serpentinization of ultramafic rocks occur. Indications of abiotic gas occurrences are therefore sparse and much speculated upon. Here, we investigated the Spitsbergen Transform Fault, the Molloy Ridge, the Molloy Deep, and the Molloy Transform Fault/Fracture Zone, (a transform fault-bounded pull-a-part region offshore western Svalbard) where both processes may be active. Multiple acoustic gas flares, ~1,770 and ~3355 m high above the seafloor (tallest ever recorded), were observed indicating active migration and seepage of hydrocarbons. The proximity to the mid oceanic ridge and the documented high heat flow suggests the influence of high temperatures on organic-rich sedimentary deposits. Deep seismic data and other geological information available indicate that the main source of gas could be from thermal cracking of either pre- or syn-rift source rock organic material, potentially mixed with methane from serpentinization of mantle rocks (peridotites). Correlation with seismic stratigraphy from Ocean Drilling Program (ODP) Sites 910 and 912 on the adjacent Yermak Plateau suggests that the sedimentary source rocks may be present at the northern flank of the Molloy Ridge and within the deep graben along the Spitsbergen Transform Fault. The ~3 km thick sedimentary succession in high heat flow zones within the transform fault and the active bounding faults allow generation and migration of hydrocarbons to the seafloor and sustains present day seepage.

KEYWORDS

gas flare, Molloy Ridge, fluid flow, multibeam, Molloy Deep, deep seismic data

Introduction

Biotic and abiotic processes in sediments lead to the generation and release of hydrocarbons through the seafloor. Biotic gas generation occurs through degradation of organic carbon in sediments through microbial and thermogenic processes (e.g., Milkov

and Etiope, 2018) whereas abiotic gas generation occurs through serpentinization of ultramafic rocks in the presence of water by Fischer-Tropsch-type reactions (Proskurowski et al., 2008). Abiotic methane generation requires circulation of seawater to mantle level and is therefore limited to locations where mantle rocks are shallow or even exposed at the seafloor (Kandilarov et al., 2008). The serpentinization rates are maximal at temperatures between 200°C and 350°C (Martin and Fyfe, 1970) and the process continues for long time periods generating enough methane to have a sustained gas supply. Slow spreading ridges are therefore suggested to be the best locations for elevated methane generation since the mantle remains at shallower depth within the relevant temperature window for a longer time (Charlou et al., 2010). In magma-limited slow and ultra-slow spreading ridges and transform faults, serpentinization occurs along detachment faults which form at young oceanic crust near the active ridge axis and over a period of 1–4 million years (Tucholke et al., 1998; Cannat et al., 2010). Biotic methane generation can also occur with the presence of organic material either through microbial and/or by thermogenic processes since one of these settings could be present due to normal microbial degradation or thermal cracking due to high heat flow.

Our study area is located in the central Fram Strait between Svalbard and Greenland (Figure 1, inset). The Fram Strait is known as the Arctic-Atlantic Gateway between the Norwegian-Greenland Sea and the Arctic Ocean and plays a key role in the deep-water exchange between the Atlantic and Arctic oceans (Hunkins, 1990; Tesi et al., 2021; von Appen et al., 2015). The Molloy Ridge and the Molloy Transform Fault and Fracture Zone System was formed well after the opening of the Norwegian-Greenland Sea ~56 Ma ago (Talwani and Eldholm, 1977). Engen et al. (2008) suggest an early age of ~19.6 Ma for the start of seafloor spreading at the present Molloy Ridge, which coincides with the recent modelling results suggesting 20 Ma for the opening of the Arctic-Atlantic Gateway (Dumais et al., 2021). In this region, the oceanic crust is thin, and the Moho is shallow (<5 km below seafloor) (Czuba et al., 2005). The Molloy Deep is the nodal basin at the intersection of the Molloy Ridge and the Molloy Transform Fault (MTF) (Klenke and Schenke, 2002). The Spitsbergen Transform Fault (STF) in the north and the MTF in the south acts as the boundaries separating the Molloy Ridge spreading zone from the rest of the spreading system further north and south, respectively (Figure 1 inset). The STF also acts as the boundary separating the pre-rift continental sedimentary rocks in the north beneath the SW flank of the Yermak Plateau from the Molloy Ridge spreading oceanic crust and sedimentary deposits further in the south. The Molloy Ridge has three segments with two blocks of highly fractured material filling the space in between and a further deformed zone west of it (Figure 1).

In this study we analysed water column acoustic and seismic reflection data to understand the source and origin of the detected gas flares in the water column, the processes behind the formation of the gases, and the resulting seepage into the water column. The possibility of different mechanisms acting together are critically analysed based on the stratigraphic information available from the nearby Ocean Drilling Program (ODP) Leg 151 boreholes and deep seismic data.

Materials and methods

Seafloor mapping using a multibeam echosounder system (MBES) across the deepest zone of the Norwegian-Greenland Sea, the Molloy Deep (up to 5,569 m deep) and surrounding areas was carried out as part of the MAREANO (mareano.no) program in 2019. The multibeam data were collected by DOF Subsea ship SV Geograph using a hull mounted Kongsberg EM304 MBES which also allowed to image the water column (Figure 1). The MBES transducer system for each ping sends out a fan of 512 beams to the water column and the backscattered energy is received by the transducer array. Since the survey is mainly planned for seafloor bathymetry mapping, the overlap with the nearby line is less than 10%. This results in a fan shaped data coverage with 100% coverage below the ship (nadir zone) and decreasing towards the outermost beam. This results in partial mapping of any anomalies occurring away from the nadir zone (refer Figure 1 in Thorsnes et al., 2023). The MBES operates at frequencies of 26–34 kHz and has a depth range of 10–8,000 m. The MBES data were processed for bathymetry by DOF Subsea as part of the delivery for MAREANO and for backscatter and water column anomalies by Geological Survey of Norway (NGU) to investigate the seafloor and water column. QPS maritime solutions FMGeocoder Toolbox and FM Midwater softwares were used to process, analyse and interpret the backscatter and water column data, respectively. The water column data were inspected visually using FM Midwater where the water column backscattering intensity is filtered to remove background noise. This process will single out higher intensity anomalies from gas flares which are then visible on the inline fan of beams and across line stack (all beams) of data.

Sub bottom profiler (SBP) shallow seismic data was collected using Kongsberg SBP 29 system which operates in the 2–9 kHz frequency range. The MBES receiver array was used to record the data. SBP data were collected across the Molloy Ridge and surrounding seafloor showing the shallow subsurface covering the entire bathymetric range and tectonic regions of the seafloor. Airgun 2D seismic reflection data were acquired by the Alfred Wegener Institute (AWI) and partners during cruise MSM31 onboard R/V Maria S. Merian in 2013. A source array of 6 G guns (each 8 L) and a 3,000 m long digital streamer were deployed (Geissler et al., 2014a). The seismic data are used to define the geological structure across the STF including the northern flank of the Molloy Ridge. The shallow sedimentary cover is seismo-stratigraphically interpreted using the tie towards the nearby ODP sites 910 and 912 (Figure 1) (Spiegler, 1996; Mattingsdal et al., 2014) to provide stratigraphic constraints on sedimentary deposition and development before and after the opening of the Arctic-Atlantic Gateway.

Results

The Molloy Ridge is located between STF and MTF (Figure 1). The Molloy Ridge is a well-developed core complex (Chamov et al., 2010; Thorsnes et al., 2023), with the shallowest part in the centre at ~1,500 m below sea level (Figure 2). The Molloy Ridge core complex includes an oceanic detachment fault forming a hanging

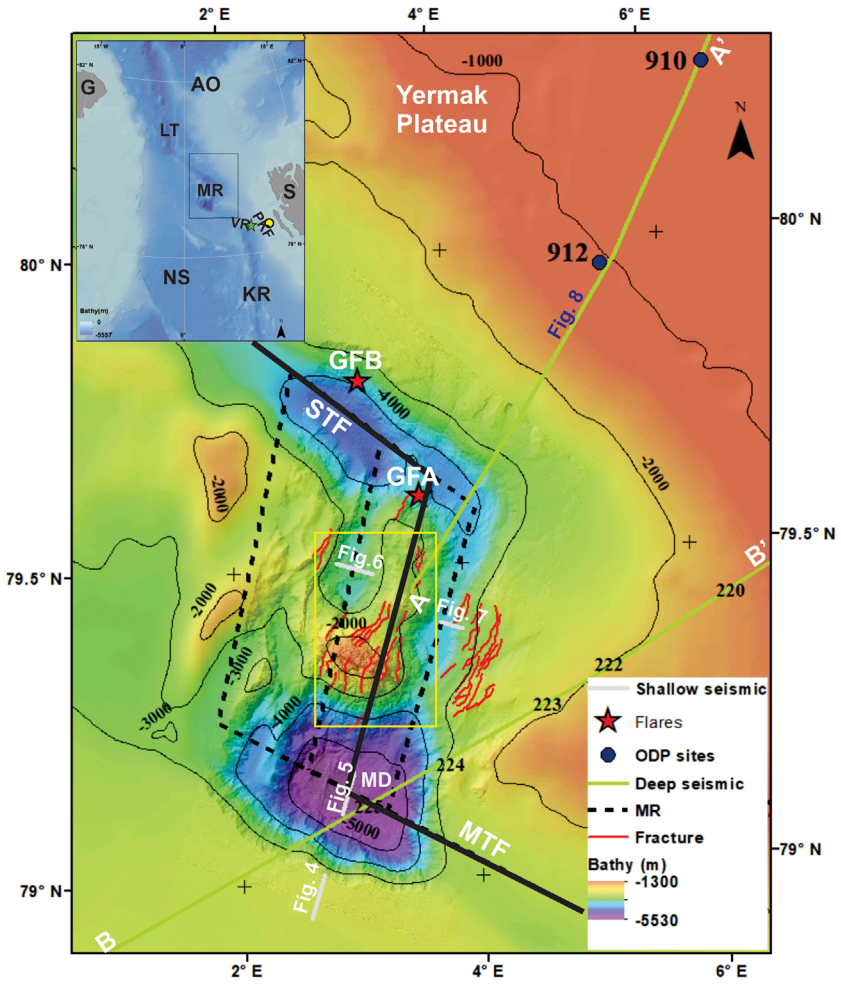

FIGURE 1
Detailed bathymetry of the study area showing faults (red lines), gas flares (red stars; GFA & GFB) and the location of ridge axis (black line) overlayed on regional (IBCAO) and detailed bathymetry. SBP and 2D seismic data are indicated by light grey and light green lines respectively. Seismic line (A-A′) is given Figure 8 and (B-B′) shows the location of seismic line from Czuba et al. (2005). Location of Figure 2 is shown as yellow box. Inset figure shows the locations of the samples in Figure 9 (red dots) from Vestnesa Ridge (VR) and Prins-Karls Forland (PKF). Also shown are the Molloy Ridge/Fracture Zone (MR), Molloy Transform Fault (MTF), Spitsbergen Transform Fault (STF), Molloy Deep (MD), Greenland (G), Norwegian-Greenland Sea (NS), Arctic Ocean (AO), Svalbard (S), Lena Trough (LT) and Knipovich Ridge (KR). Detailed bathymetry supplied by MAREANO/Norwegian Mapping Authority.

wall cut off, a corrugated surface with fault striations and steep brittle fault scarps (Figure 2). Analysis of multibeam data indicates a very complex seafloor with many fractures running parallel to the ridge axis (Figure 1). The presence of numerous slide structures visible along both sides of the Molloy Ridge and Molloy Deep indicates a tectonically very active region with high seismicity (Keiding et al., 2018) (Figure 2). The Molloy Deep, with the deepest part of the area at 5,569 m, ~3,300 m deeper than the surrounding seabed, extends about 15 km x 15 km in dimension (Figure 1).

Two water column acoustic anomalies, GFA and GFB (Figure 1), ~1770 and ~3,355 m high above the seafloor were identified (Thorsnes et al., 2023). They are located at the northern flank of the Molloy Ridge and on the conjugate side of the STF (Figure 3). Stack and fan views of the GFA (Figures 3A,B) and GFB anomalies (Figures 3C,D) show that the GFA anomaly is visible stopping within half-way through in the water column due to lack of MBES coverage in the upper water column and similarly, the top part of the GFB anomaly is also missing. The southern GFA anomaly is close to a fault mapped from the bathymetry data (Figure 1). The water column acoustic anomalies are classic indicators of gas bubble rise through the water column data (e.g., Chand et al., 2016) and verified by AUV and ROV observations (e.g., Chand et al., 2016). The deepest part of the area, the Molloy Deep, does not show any acoustic indications of fluid escape.

SBP data from the region indicate continuous sedimentation during recent times including the basinal part and the depression slopes (Figures 4–7). The sediments occur as stratified layers along the basin flanks (Figure 4) and the deepest parts of the basin (Figure 5). Fault-bounded sub-basins along the Molloy Ridge also contain stratified sediments (Figures 6, 7). The western sub-basin of the Molloy Ridge is tectonically active as indicated by the folding and faulting of stratified sediments up to the seafloor (Figure 6) compared to the eastern sub basin (Figure 7). 2D

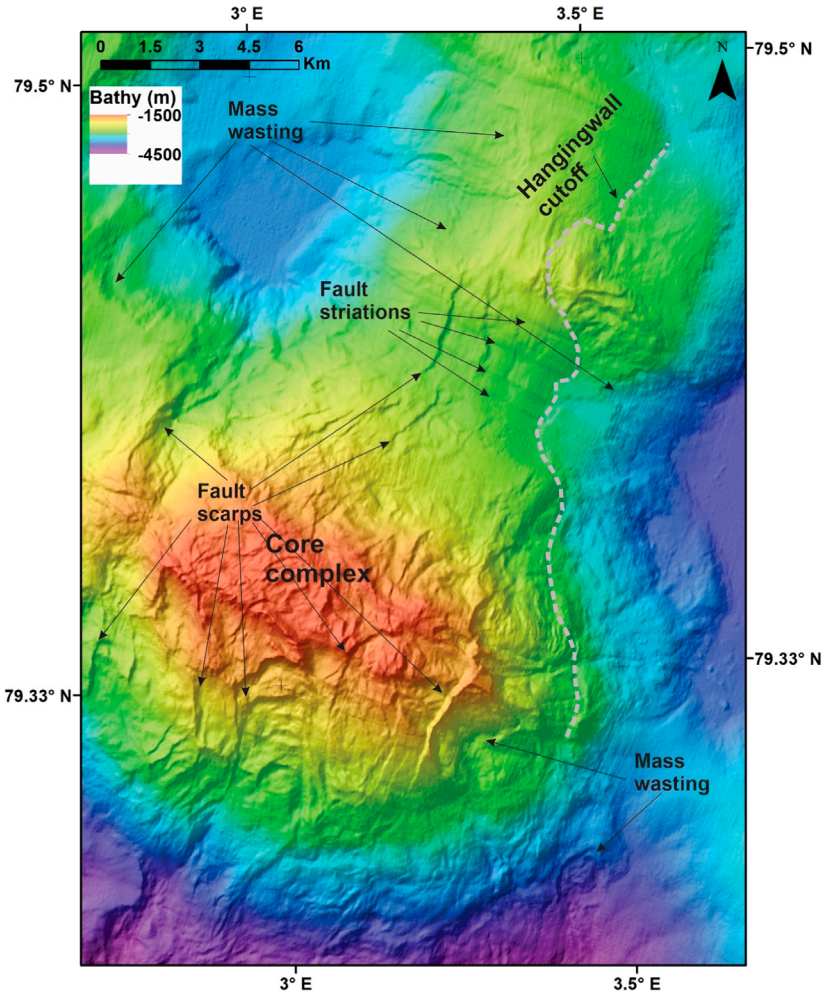

FIGURE 2
Shaded relief bathymetry image showing close-up of the Molloy core complex. The ridge is about 1,000 m high with a hanging wall cut-off, fault striations, fault scarps and mass wasting. Notice is the change in seafloor morphology with the rugged seafloor at core complex changing to smooth seafloor north of it. Detailed bathymetry supplied by MAREANO/Norwegian Mapping Authority. Location shown in Figure 1.

deep seismic data image stratified sediments on the northern flank of the STF (Figure 8). The seismic stratigraphy is traced back towards the northeast along the seismic line and two horizons are correlated with ages ~2.6 and ~5.8 Ma following Mattingsdal et al. (2014) chronostratigraphic framework for the region. The sedimentary succession at the southwestern Yermak Plateau towards STF exhibit similar character to the undisturbed sediments further northeast where they are tied to ODP sites 910 and 912 (Figure 8). A thick succession of sediments extending all the way to the STF can be observed below the 5.8 Ma horizon indicating a high sedimentation rate since the early opening of the Arctic-Atlantic Gateway (Figure 8). The deeper sediments overlying the down faulted segments towards the STF indicate the presence of pre and syn rift sediments on either side of the STF (Figure 8B). Along the seismic profile, the STF itself is covered by more than 3 km of sediments (estimated based on the velocity model in Czuba et al., 2005) with crustal level faults extending all the way up to the seafloor (Figure 8B). The sediments south of the STF flank the Molloy Ridge core complex and thins actually out on to the core complex (Figure 8B). This boundary demarcating the core complex and sediments is clearly visible on bathymetry (Figures 1, 2) where the morphological characteristics changes from very smooth surface in the north to rugged surface in the south. The projected locations of both flares GFA and GFB occurs along the region of deep-seated faults/near vertical sedimentary stratigraphic boundaries interpreted on seismic data (Figure 8).

Discussion

Morphology and gas seepage

The study area consists of a combination of ridge spreading and transform faulting along multiple segments creating a complicated seafloor morphology as well as subsurface structure. The shallow subsurface at the eastern corner of the STF is characterized by stratified sequences within a contourite drift that extends all the

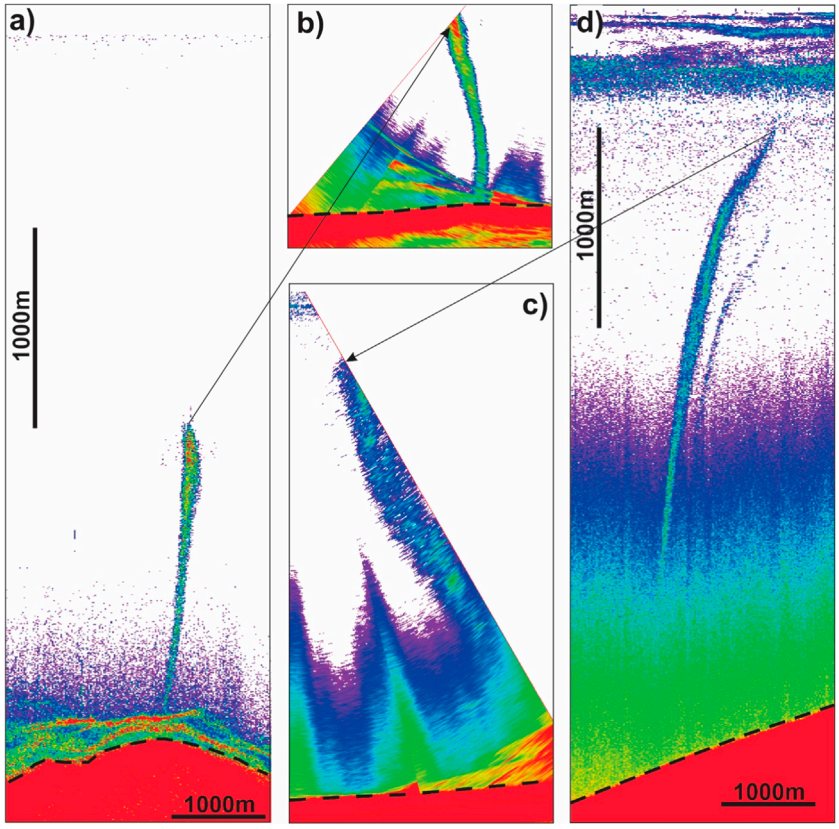

FIGURE 3
Across-track (stack of all beams) and along-track fan (stack of 25 along track pings) views respectively of acoustic gas flares GFA **(A,B)** and GFB **(C,D)**. Notice that the flare GFA is visible only up to half-way through the water column due to the lack of data in the upper part of the water column **(B)**. Similarly, the top part of the GFB is also missing **(C)**. The seafloor is indicated by black dashed line.

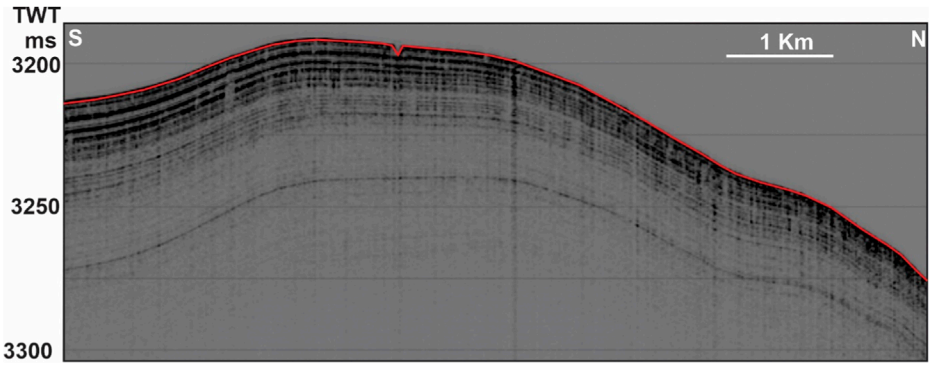

FIGURE 4
SBP line along the southern flank of the Molloy Deep showing the unfaulted stratified units (see Figure 1 for location). SBP data: MAREANO/NGU.

way into the Molloy Ridge associated basins (e.g., Osti et al., 2019). Along the peripheries of Molloy Ridge, more transparent and chaotic facies are observed indicating various episodes of sediment sliding and deformation. This is suggested to be controlled by neotectonics, changes in oceanographic conditions and fluid dynamics among the most likely processes (e.g., Elger et al., 2018; Osti et al., 2019). Submarine sliding is reported along the eastern flank of Molloy Ridge indicating triggering mechanisms mostly from gravitational instability. The latter results from the occurrence of intercalated sedimentary units with differing sedimentary architecture, which is evident in seismic data also (Czuba et al., 2005). At the steepest parts of the northern flank, the shallow sub-surface sediments are

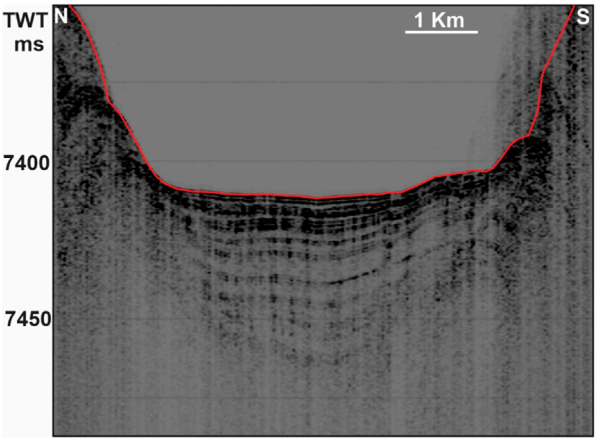

FIGURE 5
SBP line from the Molloy Deep showing the presence of stratified units covering the deepest part of the seafloor (see Figure 1 for location). SBP data: MAREANO/NGU.

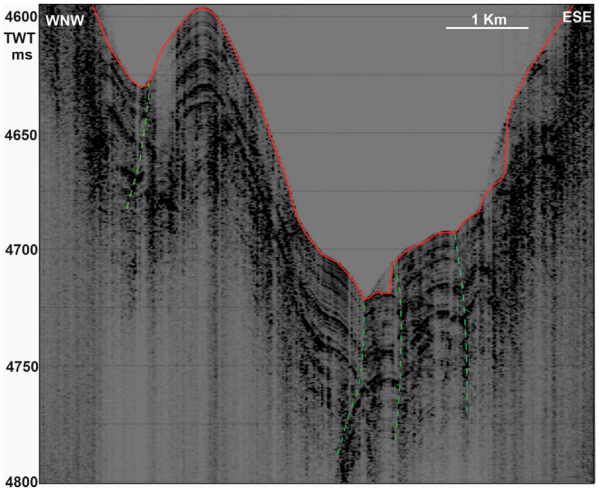

FIGURE 6
SBP line along the western depression of N-S segment of the Molloy Ridge/Fracture Zone showing the presence of heavily faulted and folded stratified units covering the fracture zone (see Figure 1 for location). Green dashed lines indicate faults. SBP data: MAREANO/NGU.

pierced by faults that seemingly extend all the way to the basement (Figure 8). The subsurface sedimentary structure could also consist of pre- and syn-rift sediments at the location of the northernmost flare (GFB) (Figure 8). The 2D deep seismic line (Figure 8) across the northern flank of STF shows pull apart rotated fault segments (pull-apart basin from syn-rift tectonics) containing these sediments and therefore it is likely that similar sediments exist in the relatively undisturbed northern part of the Molloy Ridge (south of STF) (Figure 1). This is suggested by the morphology of the ridge, whereas the southern part of Molloy Ridge consists of rugged seafloor due to a core complex exposed on the seafloor, whereas the northern segment of the ridge is smooth, comparable to normal sediment covered seafloor (Figure 1).

A gas hydrate stability zone (GHSZ) of up to 250 m thickness had been predicted for the flanks of the Molloy Ridge and the region north of STF with varying thickness related to heat flow in different parts of the region (Geissler et al., 2014b). However, a gas hydrate related bottom simulating reflection (BSR) is not visible at the flanks of the STF pull-apart basin (Figure 8). This is consistent with models that predict a non-existent or close to zero gas hydrate stability zone thickness (GHSZ) at the Molloy Ridge and STF boundary region due to high heat flow values (Geissler et al., 2014b). Nevertheless, BSR mapping in the region (Geissler et al., 2014b; Dumke et al., 2016; Osti., et al., 2017; Elger et al., 2018) suggests the existence of a gas hydrate system. Due to high heat flow being near to the mid-ocean ridge (as high as 120 mW/m^2, Klitzke et al., 2016), the thermal gradient could be high thereby proofing high temperatures as we go deep into the sediments assisting the thermal cracking of the organic matter to both gaseous and even liquid hydrocarbons. The flares are located along the peripheries of the Molloy Ridge and along the boundary faults of the STF indicating some influence of fluid flow channelling towards the margin of the ~3 km (based on velocity model from Czuba et al., 2005) thick sediment filled transform fault depression both through boundary faults and stratigraphic boundaries flanking the STF margins. The gas flares GFA and GFB could reach sea surface owing to the high acoustic strength observed at the heights they are cut off in the present data (Figure 3). However, we do not have yet proof by hydro-acoustic or satellite data.

The origin of the seeping gas in Molloy Ridge

Pull-a-part basin structures consisting potentially of pre-rift sedimentary rocks overlayed by syn-rift deposits are observed at the northern flank of STF along the 2D seismic line (Figure 8) suggesting also the presence of syn-rift sediments within the Molloy Ridge and STF area. The deeper sediments here can be seismically correlated to be clearly older than 5.8 Ma based on nearby ODP Sites 910 and 912 (Mattingsdal et al., 2014; Osti et al., 2019). The extension of thick syn-rift sediments, as continuous reflectors on pull-a-part blocks (Figure 8), indicate that the deposition of these sediments continued while the rifting was active. The deep-seated faults could be the reactivated elements from the rifting stage like those observed in analog models and other comparable pull-a-part margins (e.g., Athos and Dungun fault zones [Dooley and McClay, 1997]). The 3D structure of these faults could be even more complicated and therefore the fluid flow along these routes difficult to envisage with just a 2D imaging.

Thorsnes et al. (2023) reported condensate oil seeping gas from the seabed nearby the southern gas flare (GFA). This observation excludes a primary microbial gas origin from CO_2 reduction and methyl-type fermentation, but rather points to secondary microbial gases generated during petroleum biodegradation and thermogenic processes (Whitaker, 1999). Thermogenic gas composition can be delineated in early mature, oil-associated, and late mature thermogenic gas (Milkov and Etiope, 2018). The composition of the so far analysed free seeping gas in

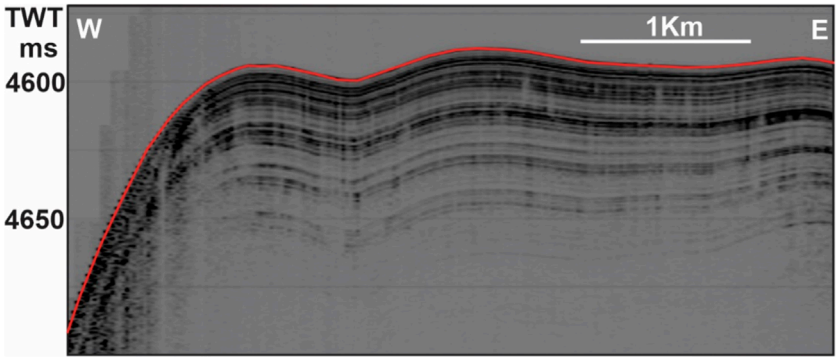

FIGURE 7
SBP line along the eastern depression of N-S segment of Molloy Ridge/Fracture Zone showing the presence of stratified units covering the seafloor. (see Figure 1 for location). SBP data: MAREANO/NGU.

the wider study region including the Vestnesa Ridge, a deep-water gas hydrate system (Plaza-Faverola et al., 2015; 2017), and the oil-seeping gas flare area off Prins Karls Forland, western Svalbard (Panieri et al., 2024) unequivocally point towards the area of oil-associated gas origin (Figure 9). The gas composition from the sub-seafloor on Vestnesa Ridge (δ^{13}C-CH_4: −51.1‰, δ^2H-CH_4: −191‰) (Plaza-Faverola et al., 2017) and oil seeps off Prins Karls Forland (δ^{13}C-CH_4: −48.4‰, δ^2H-CH_4: −196‰ (Panieri et al., 2024), are nearly identical (Figure 9) pointing towards the same petroleum system for the origin of the hydrocarbons in the region.

A likely source of the ongoing gas and oil seepage in the Molloy Ridge area, on Vestnesa Ridge, and the shelf region off Prins Karls Forland could be organic-rich deposits of Middle Miocene (>16–17 Ma; Knies and Mann, 2002) or Late Miocene (>10-11 Ma; Gruetzner et al., 2022), as recovered in ODP Site 909 in the central Fram Strait, south of the Molloy Ridge. Basin modelling (with >16-17 Ma as depositional age) revealed an ongoing hydrocarbon generation potential since the Late Miocene (~6 Ma) (Knies et al., 2018) with first seepage at the seafloor occurring during the early Pleistocene (Plaza-Faverola et al., 2015; Daszinnies et al., 2021).

Based on various palaeo-reconstruction models for the region, the Molloy Ridge was established after 20 Ma (Dumais et al., 2021) and therefore the oldest post rift sediments belong to this age. Indeed, the oldest age for the sediments lying right above the syn-rift rotated blocks and extending all the way to the STF can be assigned to be approximately ~17–18 Ma using similar sedimentation rates and shelf progradation observations as proposed by Hustoft et al. (2009) and Mattingsdal et al. (2014). While immature at the borehole location (ODP Site 909) in central Fram Strait, higher heat flow (>120 mW/m^2; Klitzke et al., 2016) nearby the STF could have increased the maturity level of the organic-rich deposits allowing the expulsion of oil-associated gas in the Molloy region and elsewhere in the region over the past 6 million years until now. Indeed, recent data compilation of oil-source rock correlation for the western Svalbard continental margin indicates an unequivocal correspondence between a Miocene source rock of deltaic/terrestrial origin and oil-associated seeping gas (Mattingsdal et al., 2023). Alternatively, the recovery of organic-rich, early to middle Eocene sediments from the Lomonosov Ridge (Backman et al., 2006), has given rise to speculations that widespread, organic-rich, potential source rocks might be present across the entire Arctic Basin and its adjacent seas (Brinkhuis et al., 2006; Bujak, 2008). These strata are characterised by the widespread occurrence of large quantities of the freshwater fern Azolla deposited during the onset of the middle Eocene (~50 Ma) (Brinkhuis et al., 2006). Basin modelling indicate that this Eocene source rock is potentially prolific close to the Gakkel Ridge with high geothermal gradients (>100°C) (Mann et al., 2009). Moreover, Blumenberg et al. (2016) suggested that the early to middle Eocene source rock is in the early oil window since the Early Miocene along the northern Barents Sea continental margin. However, the kerogen type III/II derived oil seeps from the western Svalbard margin (Mattingsdal et al., 2023; Panieri et al., 2024) rather point to a deltaic/terrestrial source rock of Middle to Late Miocene age (Knies and Mann, 2002; Gruetzner et al., 2022). The potential presence of an Eocene (*Azolla*) source rock along the northern flank of the STF and towards the ODP sites is unlikely to be the source of the condensate oil seeping gas at Molloy Ridge due to its kerogen type II/I character of the organic matter (Stein, 2007).

Slow spreading ridges, and in our case along a transform fault, are proposed to have elevated methane generation and release because of serpentinization (Charlou et al., 2010; Johnson et al., 2015). The Molloy Ridge is suggested to be a slow to ultra-slow spreading ridge and therefore serpentinization could have occurred along detachment faults over a period 1–4 million years (Tucholke et al., 1998; Johnson et al., 2015). Serpentinization due to circulation of seawater into mantle level can occur due to the relatively thin sedimentary cover (<5 km) and faults extending down to mantle exist (Kandilarov et al., 2008). The crust is thinning and shallowing in the NE direction towards the Molloy Ridge and STF from the deepest part at Molloy Deep (Czuba et al., 2005) where the flares are located. Serpentinization is suggested to occur in the region below the STF and northeast of it (Czuba et al., 2005). The occurrence of the flares along the boundary of STF suggests focussing of the fluids towards

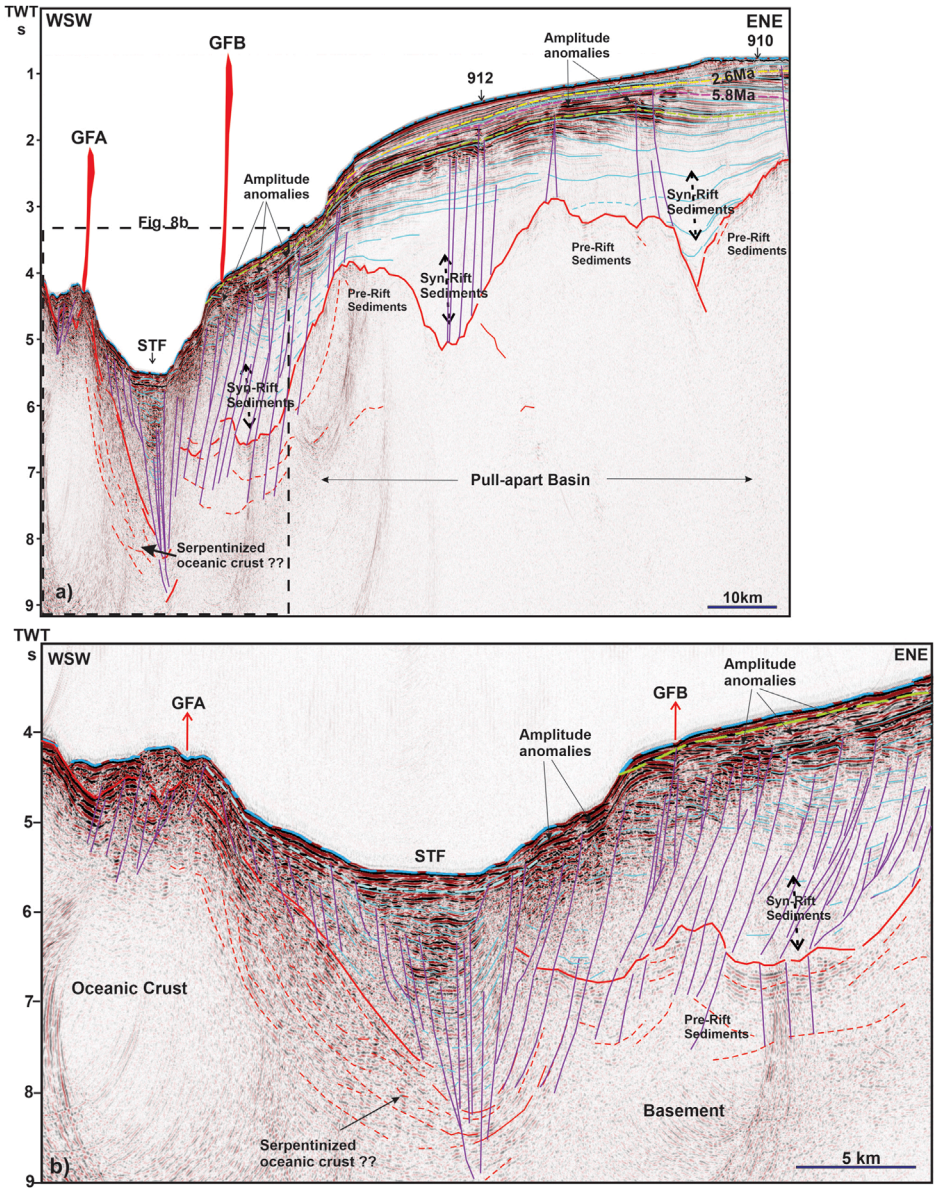

FIGURE 8
2D Seismic section (location in Figure 1) **(A)** from the northern flank of Molloy Ridge showing the pre- and syn-rift sediments along the stretched segments towards the Yermak Plateau. Stratigraphic framework derived from Mattingsdal et al. (2014) based on ODP holes 910 and 912 representing 2.6 Ma (yellow dashed line) and 5.8 Ma (purple dashed line) horizons are also shown. The horizon given in red is the acoustic basement and the sediments above extending to the STF belong to the syn-rift blocks and those deposited later. The projected location of the flare GFA (~8 km) occur along the boundary of oceanic basement towards the STF and GFB (~27 km) occurs along a bounding fault related to the STF. **(B)** Blow up of the location of gas flares and STF showing the faults and thick pack of sediments deposited in the STF. Faults are shown in purple sub-vertical lines and other horizons given in blue in both figures. Acoustic amplitude anomalies due to fluid accumulation can be seen close to boundaries of faults and connected horizons.

the transform boundary. The serpentinized zone proposed by Czuba et al. (2005) is deep but comparing the location of their seismic line (Figure 1) to STF, it is likely that the serpentinized zone could be shallow in the gas flare areas typical of transform fault boundaries where the transition is abrupt (Dooley and McClay, 1997). The gas flares are located where there is a chance for mixing between fluids seeping from different kinds of sources since the flare location is connected to the deep faults, and the transform fault is infilled by ~3 km of sediments potentially diverting the upward migrating fluids (Figure 8B). However, the contribution of abiotic methane to the seepage system may not be significant, compared to high concentrations of thermogenic methane evicted from shallower than oceanic crustal level sources (Lizzaralde et al., 2011).

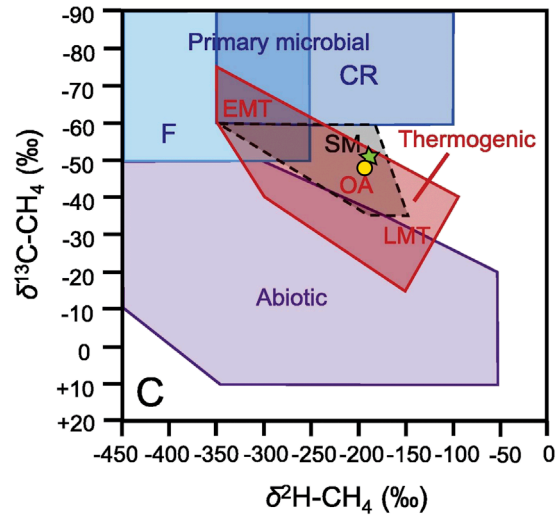

FIGURE 9
Revised methane genetic diagram based on $d^{13}C\text{-}CH_4$ and $d^2H\text{-}CH_4$ (Whiticar, 1999; Milkov and Etiope, 2018). Yellow circle: Oil-coated free seeping gas offshore Prins Karls Forland (Panieri et al., 2024), Green star: Headspace gas extracted from gravity core GC10, Vestnesa Ridge, 200 cm below seafloor (Plaza-Faverola et al., 2017). Abbreviations are: CR: CO2 reduction, F: Methyl-type Fermentation, SM: Secondary microbial, EMT: Early mature thermogenic gas, OA: Oil-associated thermogenic gas, LMT: Late mature thermogenic gas. Locations of samples are shown in Figure 1 (inset).

Currently, we cannot tell the ultimate origin for the release of gas in Molloy Ridge -STF region. More geochemical analyses and basin modelling studies are needed to clarify the source and migration pathways of the seeping hydrocarbons. Clearly, if abiogenic methane is present in the free gas bubbles, its proportions are minor and difficult to detect.

Conclusion

Gas flares rising from the seafloor into the water column from very close to an active mid-ocean ridge with potentially multiple hydrocarbon sources and source rocks offshore Svalbard is reported. The observations from the multibeam echosounder data indicate that methane is generated along the Spitsbergen Transform Fault immediately north of the slow/ultra-slow spreading Molloy Ridge and released through boundary faults of the deep sediment-filled Spitsbergen Transform Fault depression. This region is outside the gas hydrate stability zone due to high heat flow. No other locations in our data set indicated fluid seepage, including the deepest part of the area, the Molloy Deep, at the intersection of the southern part of the Molloy Ridge and the Molloy Transform Fault. The N-S oriented Molloy Ridge in-between the Spitsbergen and Molloy transform faults constitutes a highly fractured region where crustal faults reaching up to the seafloor can be observed. The high heat flow and the likely presence of Middle to Late Miocene source rocks reported from this area makes thermal cracking as the main mechanism producing oil-associated thermogenic gases most plausible, with a possibility of minor contribution from abiotic crustal/mantle sources.

Data availability statement

The datasets presented in this article are not readily available because the raw data is owned by other agencies mentioned in the manuscript. Requests to access the datasets should be directed to www.mareano.no or info.geophysics@awi.de in case of the deep seismic reflection data.

Author contributions

SC: Conceptualization, Data curation, Formal Analysis, Investigation, Methodology, Project administration, Resources, Software, Validation, Visualization, Writing–original draft. JK: Conceptualization, Data curation, Formal Analysis, Methodology, Validation, Visualization, Writing–review and editing. WG: Conceptualization, Data curation, Formal Analysis, Methodology, Software, Visualization, Writing–review and editing. AP-F: Formal Analysis, Validation, Writing–review and editing. TT: Conceptualization, Project administration, Resources, Visualization, Writing–review and editing.

Funding

The author(s) declare that financial support was received for the research, authorship, and/or publication of this article. The multibeam and SBP data were acquired through the MAREANO programme. JK is supported by the Research Council of Norway (grant #332635). AP-F is supported by the Research Council of Norway (grant #287865).

Acknowledgments

The authors thank all participants of the MAREANO programme (www.mareano.no) for invaluable cooperation. The multibeam data were acquired and supplied by the Norwegian Mapping Authority. The data is released under a Creative Commons Attribution 4.0 International (CC BY 4.0). The authors would like to thank Aspen Technology, Inc. for providing software licenses and support.

Conflict of interest

The authors declare that the research was conducted in the absence of any commercial or financial relationships that could be construed as a potential conflict of interest.

Publisher's note

All claims expressed in this article are solely those of the authors and do not necessarily represent those of their affiliated organizations, or those of the publisher, the editors and the reviewers. Any product that may be evaluated in this article, or claim that may be made by its manufacturer, is not guaranteed or endorsed by the publisher.

References

Backman, J., Moran, K., McInroy, D. B., Mayer, L. A., and the Expedition 302 Scientists (2006). Proceedings of the integrated Ocean Drilling program. *Arct. Coring Exped. (ACEX)* 302. http://publications.iodp.org/proceedings/302/302/pdf.

Blumenberg, M., Lutz, R., Schlömer, S., Krüger, M., Scheeder, G., Berglar, K., et al. (2016). Hydrocarbons from near-surface sediments of the Barents Sea north of Svalbard – indication of subsurface hydrocarbon generation? *Mar. Petroleum Geol.* 76, 432–443. doi:10.1016/j.marpetgeo.2016.05.031

Brinkhuis, H., Schouten, S., Collinson, M. E., Sluijs, A., Damste, J. S. S., Dickens, G. R., and the Expedition 302 Scientists (2006). Episodic fresh surface waters in the Eocene Arctic Ocean. *Nature* 441, 606–609. doi:10.1038/nature04692

Bujak, J. (2008). From green house to icehouse- the Azolla Trigger: implications for climate change and Arctic petroleum source rocks. *Houst. Geol. Soc. Bull.* 50 (08), 19.

Cannat, M., Fontaine, F., and Escartín, J. (2010). "Serpentinization and associated hydrogen and methane fluxes at slow spreading ridges," in *Geophysical monograph series* (Washington DC, USA: American Geophysical Union), 188. doi:10.1029/2008GM000760

Chamov, N. P., Sokolov, S. Y., Kostyleva, V. V., Efimov, V. N., Peive, A. A., Aleksandrova, G. N., et al. (2010). Structure and composition of the sedimentary cover in the Knipovich Rift valley and Molloy Deep (Norwegian-Greenland basin). *Lithology Mineral Resour.* 45, 532–554. doi:10.1134/s0024490210060039

Chand, S., Cremiere, A., Lepland, A., Thorsnes, T., Brunstad, H., and Stoddart, D. (2016). Long term fluid expulsion revealed by carbonate crusts and pockmarks connected to subsurface gas anomalies and palaeo-channels in the central North Sea. *Geo. Mar. Lett.* 37, 215–227. doi:10.1007/s00367-016-0487-x

Charlou, J. L., Donval, J. P., Konn, C., Ondreas, H., Fouquet, Y., Jean- Baptiste, P., et al. (2010). "High production and fluxes of H2 and CH4 and evidence of abiotic hydrocarbon synthesis by serpentinization in ultramafic-hosted hydrothermal systems on the Mid-Atlantic Ridge, in Diversity of Hydrothermal Systems on Slow Spreading Ocean Ridges," in *Geophys. Monogr. Ser*. Editors P. Rona, C. Devey, J. Dyment, and B. Murton (Washington, DC, USA: AGU), 188, 265–296. doi:10.1029/2008GM000752

Czuba, W., Ritzmann, O., Nishimura, Y., Grad, M., Mjelde, R., Guterch, A., et al. (2005). Crustal structure of northern Spitsbergen along the deep seismic transect between the Molloy Deep and Nordaustlandet. *Geophys. J. Int.* 161, 347–364. doi:10.1111/j.1365-246x.2005.02593.x

Daszinnies, M., Plaza-Faverola, A., Sylta, Ø., Bünz, S., Mattingsdal, R., Tømmerås, A., et al. (2021). The Plio-Pleistocene seepage history off western Svalbard inferred from 3D petroleum systems modelling. *Pet. Geol.* 128, 105023. doi:10.1016/j.marpetgeo.2021.105023

Dooley, T., and McClay, K. (1997). Analog modeling of pull-apart basins. *AAPG Bull.* 81, 1804–1826. doi:10.1306/3b05c636-172a-11d7-8645000102c1865d

Dumais, M. A., Gernigon, L., Olesen, O., Johansen, S. E., and Bronner, M. (2021). New interpretation of the spreading evolution of the Knipovich Ridge derived from aeromagnetic data. *Int.* 224, 1422–1428. doi:10.1093/gji/ggaa527

Dumke, I., Burwicz, E. B., Berndt, C., Klaeschen, D., Feseker, T., Geissler., W. H., et al. (2016). Gas hydrate distribution and hydrocarbon maturation north of the Knipovich Ridge, western Svalbard margin. *J. Geophys. Res. Solid Earth* 121, 1405–1424. doi:10.1002/2015JB012083

Elger, J., Berndt, C., Rupke, L., Krastel, S., Gross, F., and Geissler, W. H. (2018). Submarine slope failures due to pipe structure formation. *Nat. Comm.* 9, 715. doi:10.1038/s41467-018-03176-1

Engen, Ø., Eldholm, O., and Bungum, H. (2003). The Arctic plate boundary. *Geophys Res.* 108 (B2), 2075. doi:10.1029/2002JB001809

Engen, Ø., Faleide, J. I., and Dyreng, T. K. (2008). Opening of the Fram Strait gateway: a review of plate tectonic constraints. *Tectonophysics* 450, 51–69. doi:10.1016/j.tecto.2008.01.002

Escartin, J., Mevel, C., Petersen, S., Bonnemains, D., Cannat, M., Andreani, M., et al. (2017). Tectonic structure, evolution, and the nature of oceanic core complexes and their detachment fault zones (13°20′N and 13°30′N, Mid Atlantic Ridge). *Geochem. Geophys. Geosys.* 18, 1451–1482. doi:10.1002/2016GC006775

Geissler, H. W., Gebhardt, C. A., and Schmidt-Aursch, C. M. (2014a). The Hinlopen/Yermak Megaslide (HYM) – understanding an exceptional submarine landslide, its consequences and relation to the deep structure of the Sophia Basin (Sophia-HYM) – cruise No. MSM31 – august 17 – september 18, 2013 – tromsø (Norway) – bremen (deutschland). *DFG-Senatskommission für Ozeanogr.* 31, 70. MARIA S. MERIAN Berichte. doi:10.2312/cr_msm31

Geissler, W. H., Pulm, P. V., Jokat, W., and Gebhardt, A. C. (2014b). Indications for the occurrence of gas hydrates in the Fram Strait from heat flow and multichannel seismic reflection data. *J. Geol. Res.* 2014, 1–12. doi:10.1155/2014/582424

Gruetzner, J., Matthiessen, J., Geissler, W. H., Gebhardt, C., and Schreck, M. (2022). A revised core-seismic integration in the Molloy Basin (ODP Site 909): Implications for the history of ice rafting and ocean circulation in the Atlantic-Arctic gateway. *Global and Planetary Change*. 215. doi:10.1016/j.gloplacha.2022.103876

Hunkins, K. (1990). "A review of the physical oceanography of Fram Strait," in *The physical oceanography of sea straits*. Editor L. R. Pratt (Dordrecht, Netherlands: Springer), 61–94.

Hustoft, S., Bünz, S., Mienert, J., and Chand, S. (2009). Gas hydrate reservoir and active methane-venting province in sediments on <20Ma young oceanic crust in the Fram Strait, offshore NW-Svalbard. *Earth. Planet. Sci. Lett.* 284, 12–24.

Johnson, J. E., Mienert, J., Plaza-Faverola, A., Vadakkepuliyambatta, S., Knies, J., Buenz, S., et al. (2015). Abiotic methane from ultraslow-spreading ridges can charge Arctic gas hydrates. *Geology* 43, 371–374. doi:10.1130/G36440.1

Kandilarov, A., Mjelde, R., Okino, K., and Murai, Y. (2008). Crustal structure of the ultra-slow spreading Knipovich Ridge, North Atlantic, along a presumed amagmatic portion of oceanic crustal formation. *Mar. Geophys. Res.* 29 (2), 109–134. doi:10.1007/s11001-008-9050-0

Keiding, M., Olesen, O., and Dehls, J. (2018). Neo tectonic map of Norway and adjacent areas, Geological Survey of Norway. https://www.ngu.no/upload/Publikasjoner/Kart/Neotectonic_Map_NGU.pdf.

Klenke, M., and Schenke, H. W. (2002). A new bathymetric model for the central Fram Strait. *Mar. Geophys. Res.* 23, 367–378. doi:10.1023/a:1025764206736

Klitzke, P., Sippel, J., Faleide, J. I., and Scheck-Wenderoth, M. (2016). A 3D gravity and thermal model for the Barents Sea and kara sea. *Tectonophysics* 684, 131–147. doi:10.1016/j.tecto.2016.04.033

Knies, J., Daszinnies, M., Plaza-Faverolla, A., Chand, S., Sylta, Ø., Buez, S., et al. (2018). Modelling persistent methane seepage offshore western Svalbard since early Pleistocene. *Mar. Pet. Geol.* 91, 800–811. doi:10.1016/j.marpetgeo.2018.01.020

Knies, J., and Mann, U. (2002). Depositional environment and source rock potential of Miocene strata from the central Fram Strait: introduction of a new computing tool for simulating organic facies variations. *Mar. Pet. Geol.* 19, 811–828. doi:10.1016/s0264-8172(02)00090-9

Lizarralde, D., Soule, S. A., Seewald, J. S., and Proskurowski, G. (2011). Carbon release by off axis magmatism in a young sedimented spreading centre. *Nat. Geosci.* 4, 50–54. doi:10.1038/ngeo1006

Mann, U., Knies, J., Chand, S., Jokat, W., Stein, R., and Zweigel, J. (2009). Evaluation and modelling of Tertiary source rocks in the central Arctic Ocean. *Mar. Pet. Geol.* 26, 1624–1639. doi:10.1016/j.marpetgeo.2009.01.008

Martin, B., and Fyfe, W. S. (1970). Some experimental and theoretical observations on the kinetics of hydration reactions with particular reference to serpentinization. *Chem. Geol.* 6, 185–202. doi:10.1016/0009-2541(70)90018-5

Mattingsdal, R. (2023). "A new young source rock offshore western Svalbard proven with oil seep geochemical results – possible regional implication for the westernmost Barents Sea," in Norwegian Petroleum Directorate, Petroleum Systems Conference, Oslo, Norway.

Mattingsdal, R., Knies, J., Andreassen, K., Fabian, K., Husum, K., Grøsfjeld, K., et al. (2014). A new 6 Myr stratigraphic framework for the Atlantic-Arctic Gateway. *Quart. Sci. Rev.* 92, 170–178. doi:10.1016/j.quascirev.2013.08.022

Milkov, A. V., and Etiope, G. (2018). Revised genetic diagrams for natural gases based on a global dataset of >20000 samples. *Org. Geochem.* 125, 109–120. doi:10.1016/j.orggeochem.2018.09.002

Osti, G., Franek, P., Forwick, M., and Laberg, J. S. (2017). Controlling factors for slope instability in a seismically active region: the NW-Svalbard continental margin. *Mar. Geol.* 390, 131–146. doi:10.1016/j.margeo.2017.06.005

Osti, G., Waghorn, K. A., Waage, M., Plaza-Faverola, A., and Ferre, B. (2019). Evolution of contourite drifts in regions of slope failures at eastern Fram Strait. *Arktos* 5, 105–120. doi:10.1007/s41063-019-00070-y

Panieri, G., Argentino, C., Ramalho, S. P., Vulcano, F., Savini, A., Fallati, L., et al. (2024). An Arctic natural oil seep investigated from space to the seafloor. *Sci. Total Environ.* 907, 167788. doi:10.1016/j.scitotenv.2023.167788

Panieri, G., Knies, J., Vadakkepuliyambatta, S., Lee, A. L., and Schubert, C. J. (2023). Evidence of Arctic methane emissions across the mid Pleistocene. *Commun. Earth Environ.* 4, 109. doi:10.1038/s43247-023-00772-y

Plaza-Faverola, A., Bunz, S., Johnson, J. E., Chand, S., Knies, J., Mienert, J., et al. (2015). Role of tectonic stress in seepage evolution along the gas hydrate-charged Vestnesa Ridge, Fram Strait. *Geophys. Res. Lett.* 42, 733–742. doi:10.1002/2014GL062474

Plaza-Faverola, A., and Keiding, M. (2019). Correlation between tectonic stress regimes and methane seepage on the western Svalbard margin. *Solid earth.* 10, 79–94. doi:10.5194/se-10-79-2019

Plaza-Faverola, A., Vadakkepuliyambatta, S., Hong, W.-L., Mienert, J., Bünz, S., Chand, S., et al. (2017). Bottom-simulating reflector dynamics at Arctic thermogenic

gas provinces: an example from Vestnesa Ridge, offshore west Svalbard. *J. Geophys. Res. Solid Earth* 122, 4089–4105. doi:10.1002/2016JB013761

Proskurowski, G., Lilley, M. D., Seewald, J. S., Früh-Green, G. L., Olson, E. J., Lupton, J. E., et al. (2008). Abiogenic hydrocarbon production at Lost City hydrothermal field. *Science* 319 (5863), 604–607. doi:10.1126/science.1151194

Rajan, A., Mienert, J., Bünz, S., and Chand, S. (2012). Potential serpentinization, degassing, and gas hydrate formation at a young (<20 Ma) sedimented ocean crust of the Arctic Ocean ridge system. *Jour. Geophys. Res.* 117, B03102. doi:10.1029/2011JB008537

Spiegler, D. (1996). "Planktonic foraminifer Cenozoic biostratigraphy of the Arctic Ocean, Fram Strait (Sites 908e909), Yermak Plateau (Sites 910e912), and East Greenland Margin (Site 913)," in *Proceeding Ocean drilling program, scientific results*. Editors J. Thiede, A. M. Myhre, J. V. Firth, G. L. Johnson, and W. F. Ruddiman (College Station, Texas, USA: Ocean Drilling Program), 151, 153–167.

Stein, R. (2007). Upper Cretaceous/lower Tertiary black shales near the North Pole: organic-carbon origin and source-rock potential. *Mar. Petroleum Geol.* 24 (2007), 67–73. doi:10.1016/j.marpetgeo.2006.10.002

Talwani, M., and Eldholm, O. (1977). Evolution of the Norwegian-Greenland sea. *GSA Bull.* 88, 969–999. doi:10.1130/0016-7606(1977)88<969:eotns>2.0.co;2

Tesi, T., Muschitiello, F., Mollenhauer, G., Miserocchi, S., Langone, L., Ceccarelli, C., et al. (2021). Rapid atlantification along the Fram Strait at the beginning of the 20th century. *Sci. Adv.* 7, eabj2946. doi:10.1126/sciadv.abj2946

Thorsnes, T., Chand, S., Bellec, V., Nixon, F. C., Brunstad, H., Lepland, A., et al. (2023). Gas seeps in Norwegian waters – distribution and mechanisms. *Nor. J. Geol.* 103, 202309. doi:10.17850/njg103-2-4

Tucholke, B. E., Lin, J., and Kleinrock, M. C. (1998). Megamullions and mullion structure defining oceanic metamorphic core complexes on the Mid-Atlantic Ridge. *Jour. Geophys. Res.* 103, 9857–9866. doi:10.1029/98JB00167

von Appen, W.-J., Besczynska-Moller, A., and Fahrbach, E. (2015). Physical oceanography and current meter data from mooring F3-15. *Pangea*. doi:10.1594/PANGAEA.853902

Whiticar, M. J. (1999). Carbon and hydrogen isotope systematics of bacterial formation and oxidation of methane. *Chem. Geol.* 161, 291–314. doi:10.1016/s0009-2541(99)00092-3